A Closer Look at the Frustrated Ising Model on a Hierachical Lattice and Possible Phase Diagram Modifications

Jun Yong Khoo
Department of Physics, Massachusetts Institute of Technology
(Dated: May 16, 2014)

We review the study of competing ferromagnetic and antiferromagnetic interactions in hierachical Ising models [1] and their chaotic renormalization group trajectories assosciated with the spin-glass phase. We reproduce various plots and explicitly show that the onset of chaos (the spin-glass phase) is preceded by bifurcations of renormalization group trajectories and the rate of bifurcation converges to the Feigenbaum constant 4.6692. We present the results of our investigation on how the interplay of the various parameters in this class of models affect and determine the chaotic nature of the renormalization group trajectories, from which we made several observations that may lead to an extension of the phase diagram previously proposed in [1].

I. INTRODUCTION

Unlike on Bravais lattices, classical spin models (such as the Ising model and Potts models) on hierachical lattices are not translationally invariant. However, they form a large and diverse class of exactly soluble models. They can exhibit interesting and nonclassical phase transitions at finite temperatures. A general definition of hierachical models, as well as several examples, are provided in [2]. An illustrative example is the "diamond" hierarchical lattice, whose construction is shown Fig. 1(a). We simply replace each bond sequentially with a rhombus of bonds and repeat this procedure indefinitely. Evidently, hierachical lattices are topologically different from the usual Bravais lattices in that they are by construction, self-similar lattices. In particular, the construction scheme defining each hierachical lattice is precisely the inverse of its renormalization group scheme, and hence it is not surprising that these models are exactly soluble, since the corresponding recursion relations we get are necessarily self-similar at ever step of renormalization by construction.

The exact renormalization group transformations for certain hierarchical lattices are in fact identical to various approximate real-space renormalization group schemes traditionally applied to spin systems on Bravais lattices (e.g. Migdal-Kadanoff bond-moving scheme), implying their validity as approximations in the thermodynamic limit [2]. As such, the work we review here can be interpreted as an exact study of frustration on an unusual lattice, or as an indirect approximation to frustrated spins on Bravais lattices. What is interesting in this particular hierachical lattice proposed, is the emergence of chaotic renormalization group trajectories, which is a microscopic characteristic of the spin-glass phase.

II. REVIEW

McKay et al. showed that highly frustrated, but not necessarily random, systems with frustration at every length scale can be modelled by hierarchical Ising models on a modified form of the diamond hierachical lattice that is shown in Figs. 1(b)-(d) [1]. Each site i is occupied by a spin $\sigma_i = \pm 1$. Each straight line represents a bond with the Ising interaction energy $-\beta H_{ij} = K\sigma_i\sigma_j + G$, with $K \geq 0$ [3]. A wriggly line represents an infinite antiferromagnetic coupling, whose effect is to reverse the sign of K on its adjacent bond(s). This way of introducing competing ferromagnetic (FM) and antiferromagnetic (AFM) interactions allows us to conveniently work with only one-parameter recursions.

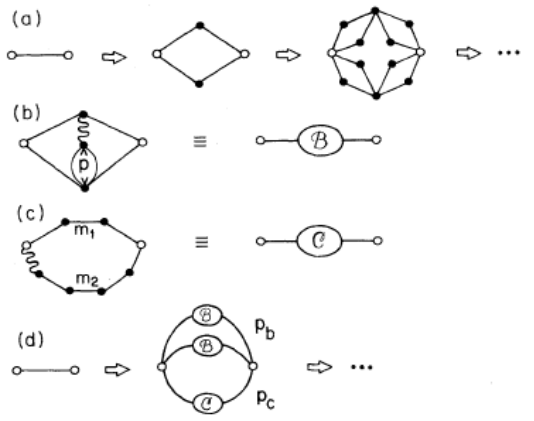

FIG. 1: The construction of hierachcical models for: (a) a "diamond lattice"; (b)-(d) the hierachical lattice Ising model

Within the unit of Fig. 1(b), p AFM bonds are in parallel. We will denote such a cluster as the 'B-bond'. The unit in Fig. 1(c) has 2 parallel chains of bonds, one made of m_1 FM bonds (and hence $m_1 - 1$ internal sites given by the black dots), and the other formed by m_2 bonds (and hence $m_2 - 1$ internal sites), all of which are FM except for the first one being AFM. We will denote such a cluster as the 'C-bond' and as representatively shown in Fig. 1(c), $m_2 > m_1$ [4]. The family of hierachical lattices employed is then constructed as per Fig. 1(d), with each bond replaced by p_b B-bonds and p_c C-bonds at each step.

The shortest path across each composite unit is defined as the length rescaling factor of the corresponding renormalization group transformation, $b = 2$. The volume rescaling factor is given by the ratio of the numbers of old and new bonds, $b^d = (4+p)p_b + (m_1+m_2)p_c$, from which we have indirectly defined the effective dimensionality d.

We rederived the renormalization group transformations and reproduce the recursion relations for the nth renormalization group iteration for the bond strength K and the constant term G below:

$$K' = p_b \tanh^{-1} \tilde{t}_b + p_c \left(\tanh^{-1} t^{m_1} - \tanh^{-1} t^{m_2} \right), \quad (1)$$

$$\begin{aligned} G' = G + b^{-dn} \Bigg\{ & [2p_b + (m_1 + m_2 - 2)p_c] \ln 2 \\ & + \frac{p_b}{2} \ln \left[\frac{(1+t^2)^2 - 4t^2\tilde{t}}{(1-t^2)^2(1-\tilde{t})^2} \right] \\ & + \frac{p_c}{2} \ln \left[\frac{(1-t^{2m_1})(1-t^{2m_2})}{(1-t^2)m_1 + m_2} \right] \Bigg\}, \end{aligned} \quad (2)$$

where $\tilde{t}_b = 2t^2(1-\tilde{t})/(1+t^4-2t^2\tilde{t})$, $t \equiv \tanh^{-1}(K)$ and $\tilde{t} \equiv \tanh^{-1}(pK)$.

We reproduce the plots shown in 'FIG. 2.' of [1] and present both in Figs. 2-3. These show a perfect match, with our plots being more resolved copies of the original due to improvement in computational power over the years. These were produced with parameters $p = 4, p_c = 1$, and $m_2 = m_1 + 1$[4] with p_b scanned at a fixed value of $m_1 = 7$ and 3, and with m_1 scanned at a fixed value of $p_b = 40$ respectively.

As pointed out in the original paper, beyond a certain threshold of m_1 and p_b, an unstable fixed point emerges at some finite coupling t_C^*, indicating a phase transition between the paramagnetic ($t < t_C^*$) and FM ordered ($t > t_C^*$) phases. The FM ordered stable fixed points have an interesting behaviour for increasing values of either m_1 or p_b. With reference to Fig. 2(a), one such fixed point emerges first at around $p_b \simeq 7$, and its value increases gradually up to $p_b = p_b(2^1) \simeq 17$, where it first bifurcates (splits) into a period-2 limit cycle. Period doubling occurs again next at $p_b = p_b(2^2) \simeq 26$, and such bifurcations continue to occur at a rate that converges to the Feigenbaum constant $\simeq 4.6692$, i.e.

$$\lim_{l\to\infty} \delta_l \equiv \lim_{l\to\infty} \frac{p_b(2^l) - p_b(2^{l-1})}{p_b(2^{l+1}) - p_b(2^l)} \simeq 4.6692, \quad (3)$$

as $p_b \to p_b(2^\infty) \simeq 31$. We numerically verify this by finding the bifurcation points $p_b(2^l)$ up to $l = 10$ and the corresponding δ_l values. We do so by considering the bifurcation points, which like other dynamical systems, the are the zeroes of the Lyapunov exponents λ over the parameter space of interest [6]. For the class of models we are considering, the parameter space is spanned by $\{p, p_b, p_c, m_1, m_2\}$, but for illustrative purposes, we restrict ourselves to $\{p_b\}$ and set the other parameters to the values used to produce Fig. 2(a). And thus for our system starting at t_0 evolving for n iterations, we have [7]

$$\lambda(p_b) \equiv \frac{1}{n} \sum_{i=0}^{n-1} \ln \left| \frac{\partial}{\partial t} t'(p_b, t_i) \right|, \quad (4)$$

where $t'(p_b, t) = \tanh(K'(p_b, t))$. A negative *lambda* indicates eventual attraction to the stable fixed points or a limit cycle, while positive λ corresponds to chaotic trajectories. In our case (Fig. 4), we see that $\lambda\left(p_b \le p_b(2^\infty)\right) \le 0$, and take positive values only beyond $p_b(2^\infty)$, corresponding to the emergence of chaotic bands of renormalization trajectories. These bands eventually merge into a single band, interupted by small distinct windows of finite-period limit cycles.

An important characteristic of the chaotic bands is their self-similarity - after the transient behaviour from the initial renormalization group transformations, the profile of the chaotic band formed by each successive group of N iterations of the renormalization group transformations becomes identical in the limit of large N [8]. Physically, this implies that a geometrically coarse-grained spin-glass phase is self-similar and a microscopic interpretation can be given as follows. Starting from an initial condition in the low-temperature regime (large t), upon repeated renormalizations, the system visits the stronger coupling region $t \gg t_c$ and the weaker coupling region $t \gtrsim t_c$ within the chaotic band in a chaotic but deterministic fashion, such that the effective coupling between spins (and hence also spin correlation) alternates between strong and weak regimes as we look at increasing separation length scales. This implies infinite subsets of non-contiguous spins, which are strongly pinned to each other within each subset and are thus highly ordered. However, spins within a subset are disordered with respect to the other subsets.

In an actual sample, frustration is caused by a quenched random spatial distribution of competing interactions. The spatial disorder causes different regions to become out of phase with each other as their respective local couplings within the chaotic band are renormalized. The disorder will introduce random noise into the system, which under renormalization, should cause the limit cycles to destabilize and hence remove them. In contrast, the chaotic behaviour would be stable to such noise [9]. With the above in mind, the authors proposed a phase diagram which we reproduce here in Fig. 5.

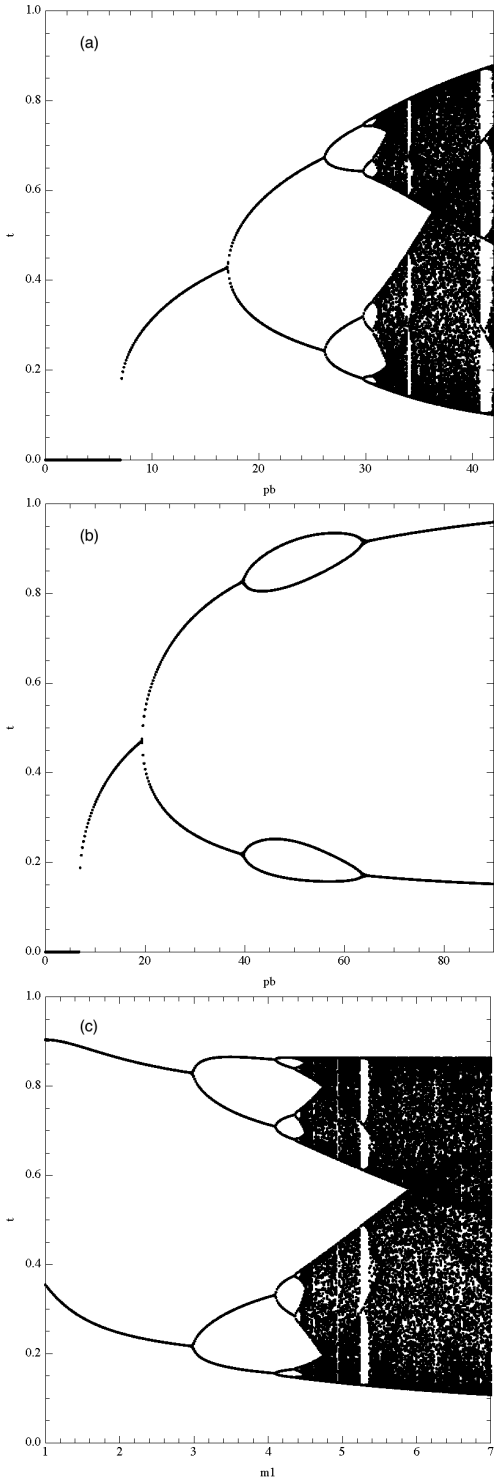

FIG. 2: Reproduced high resolution versions of the renormalization group topologies as Hamiltonian parameters are scaned, as per 'FIG. 2.' of [1], which we show in Fig. 3 for comparison. Plotted here are only the stable fixed points, limit cycles, and the space filling chaotic regions for $p = 4$, $p_c = 1$, $m_2 = m_1 + 1$. For (a) $m_1 = 7$ and (b) $m_1 = 3$, with p_b scanned; for (c) $p_b = 40$ and m_1 scanned. We also attempted to reproduce the plots in [10] but were unable to do so with the parameters provided.

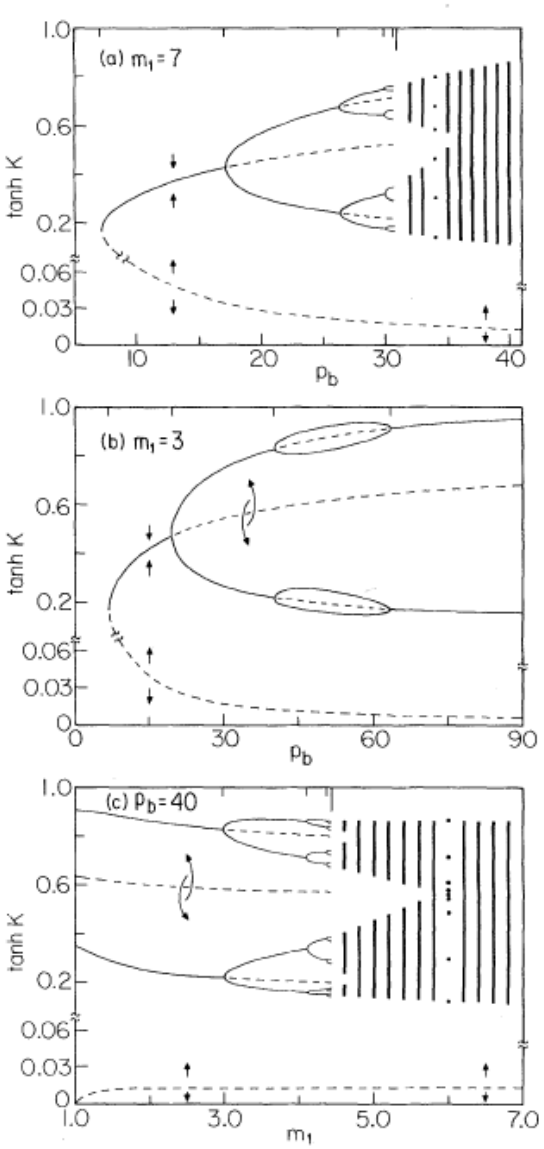

FIG. 3: Original plots from 'FIG. 2.' of [1]

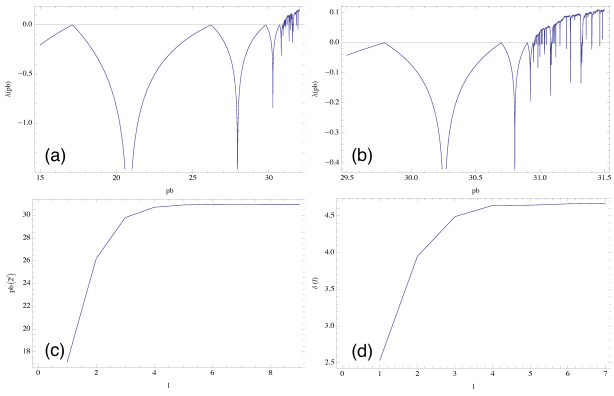

FIG. 4: Quantities associated with the renormalization group trajectory of Fig. 2(a). (a), (b) Lyapunov exponents; (c) bifurcation points $p_b(2^l)$; (d) δ_l from Eqn.3

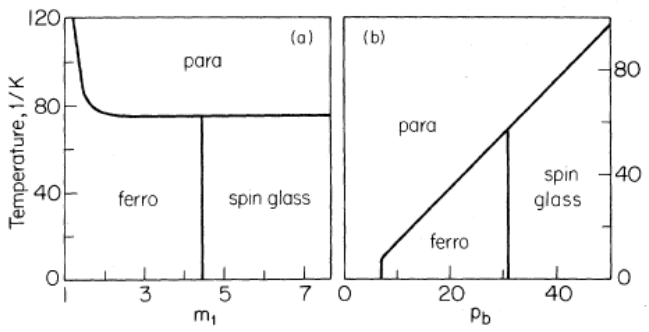

FIG. 5: Original phase diagrams deduced from (a) Fig. 2(c) and (b) Fig. 2(a).

III. INVESTIGATION OF PARAMETERS

Let us now investigate how the various parameters affect the renormalization process, and thus the phases that emerge. As mentioned in the previous section, the full parameter space is given by $\{p, p_b, p_c, m_1, m_2\}$, which is very large, and we thus skew our investigation towards what is relevant to the emergence of the chaotic renormalization trajectories.

From Eqn. 1, we see that the recursion of t (or explicitly K) is conveniently split into 2 disjoint parts, one coming solely from the B-bond contribution ('B-term') and the other from the C-bond ('C-term'), indicated by their corresponding coefficients p_b and p_c. Let us first consider their effects separately, starting with the C-term.

But before that, we first mention briefly that the B-term is strictly non-negative and always starts at 0. Furthermore, it always approaches 0 as $t \to 1$ for $p \geq 3$ as shown in Fig. 6(a). With this in mind, let us return to the C-term. Since $|t| \leq 1$, it is clear that the magnitude of the C-term increases monotonically as $t \to 1$ [11]. Thus for $p \geq 3$, in order that $K'(K) \geq 0$ always, we require that $m_2 > m_1$. We define a parameter $dm \equiv m_2 - m_1 > 0$ to implicitly account for this restriction on the m_2 parameter space.

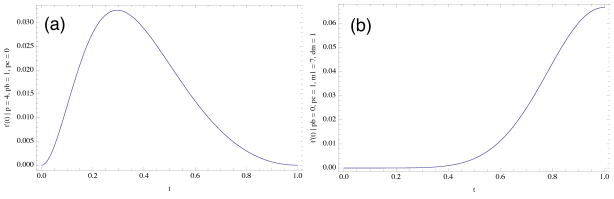

FIG. 6: (a) Plot of $t'(t)$ for $p_c = 0$, $p = 4$, and $p_b = 1$ to show effects of 1 representative B-bond unit. (b) Plot of $t'(t)$ for $p_c = 1$, $p_b = 0$, $m_1 = 7$, $dm = 1$ to show effects of 1 representative C-bond unit.

For $p_c = 1$, there is only one stable fixed point at $t = 0$ for any value of m_1 and dm. Hence only the paramagnetic phase exists here. For $p_c > 1$, an unstable fixed point appears whose position is dependent on the combination of p_c, m_1, and dm values. This just characterizes the paramagnetic to FM phase transition for our system. It is clear that for our restricted parameter space $\{p \geq 3, m_1 > 0, dm > 0\}$, the C-bonds are not responsible for the emergence of the spin-glass phase.

This leads us to conclude that the spin glass characteristic and chaotic renormalization trajectories arise solely due to the B-bonds. We illustrate this conclusion convincingly in Fig. 7(b), which was obtained for the same parameters as in Fig. 2(a) but for $p_c = 0$ to completely exclude all effects from the C-bonds. The B-bonds alone were sufficient and in fact necessary to generate chaotic trajectories. The onset of chaos occurs at $26 < p_b(2^\infty) < 27$, smaller than what we had in Fig. 2(a) with $p_b(2^\infty) \simeq 31$. This can be understood as the C-bonds suppressing the frustration provided by the B-bonds, and thus delaying the onset of the spin-glass phase.

A natural question to ask is how do the remaining parameters $\{p, p_b\}$, i.e. those associated with the B-bonds, affect the onset of chaotic trajectories. We perform a sweep in p_b for $p = 2, 4$ and present them in Figs. 7(a)-(b). From these results, it is clear that we require sufficiently large p (> 2)and p_b values for the spin-glass phase to be favorable. From Fig. 1, we expect each of their contributions to be qualitatively very different. We can think of p as a measure for the strength or intensity of frustration, and p_b as an effective density of frustrated spin clusters in our system.

From what we have discussed, we can now suggest an explanation for the absence of chaotic trajectories in the small m_1 limit even for arbitrarily large values of p_b as shown in Fig. 2(b). In this small m_1 regime, or more generically, in the regime where the C-terms are sufficiently large, the frustration effects introduced by the B-bonds are heavily suppressed by the C-bonds, causing the FM or paramagnetic phase to be more favorable than the spin-glass phase. As we tune down the strength of the C-bonds (by increasing m_1 for instance), we allow the frustration in the B-bonds to become significant again and the chaotic trajectories emerge.

The ratio p_b/p_c can then be understood as the relative densities of the B-bonds and C-bonds, as one would expect from how this lattice is constructed. The separation of magnitudes (p_b being about an order of magnitude larger than p_c) is traced back to how strongly each of the B- or C-bonds influence the strength of the renormalized coupling. This is indicated by the magnitude of the one step renormalized coupling by each of them alone as shown in Figs. 6(a)-(b). Their absolute magnitude however, plays an important role as well. For large p_c, frustration effects are heavily suppressed and we return to the paramagnetic-FM phase diagrams that we explored earlier in this section, in which case the absolute magnitude of p_c determines the location of the unstable fixed point. For large p_b however, several interesting phenomena develop. This region of the parameter space was not

discussed nor explored previously.

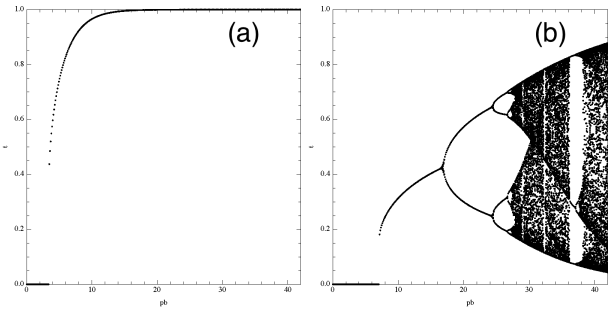

FIG. 7: Renormalization group topologies as p_b is scanned for (a) $p_c = 0$, $p = 2$, and (b) $p_c = 0$, $p = 4$, the latter showing that chaotic renormalization trajectories can be produced solely from B-bonds.

IV. EXPLORING UNCHARTERED GROUNDS: A POSSIBLE PHASE DIAGRAM EXTENSION

In this section, we will discuss three main observations that were previously unexplored. These interesting observations can potentially modify and give rise to new phase diagrams for this class of hierachical lattice Ising models beyond those proposed originally. We hereby give a brief description for each of them and their corresponding phase diagrams.

A. Direct Paramagnetic to Spin-Glass Phase Transition

This observation came from a continuation of our previous study of the B-bonds and frustration in the absence of C-bonds. We conitinue to scan the $\{p\}$ space while sweeping across the $\{p_b\}$ space and show our results in Figs. 8(a)-(e) for $6 \leq p \leq 10$. We see that as the intensity of frustration p is increased, contrary to what we might expect, it actually delays the onset of the chaotic renormalization trajectories. A larger density of B-bonds are required (despite having stronger frustration), as is indicated by the increased $p_b(2^\infty)$ value.
Furthermore, it also delays the onset of the FM phase (first non-trivial fixed point), but does so at a faster rate, thereby reducing the p_b width of the FM phase in the phase diagram of Fig. 5(b). This is shown by the decreasing p_b width of the limit cycle region in the renormalization group topologies as we increase p. The first interesting anomally is encountered at $p = 8$ where the bifurcation process is truncated, so that the trivial fixed point directly transits into a peiod-4 limit cycle. This is followed by a complete absence of the bifurcation process and a direct transition to chaos at $p = 9$, indicating a direct paramagnetic to spin-glass phase transition, and followed by the complete disappearance of ordering at $p = 10$. While we this phenomenon occurs only for a very small p_b window, but its existence suggests the feasibility of using such models as effective descriptions of certain systems that exhibit paramagnetic to spin-glass phase transitions [12].
This suggests that the spin-glass phase is a rather delicate phase. For it to be favorable over either the FM or paramagnetic phase, we cannot have frustrations that are neither too weak nor too intense.

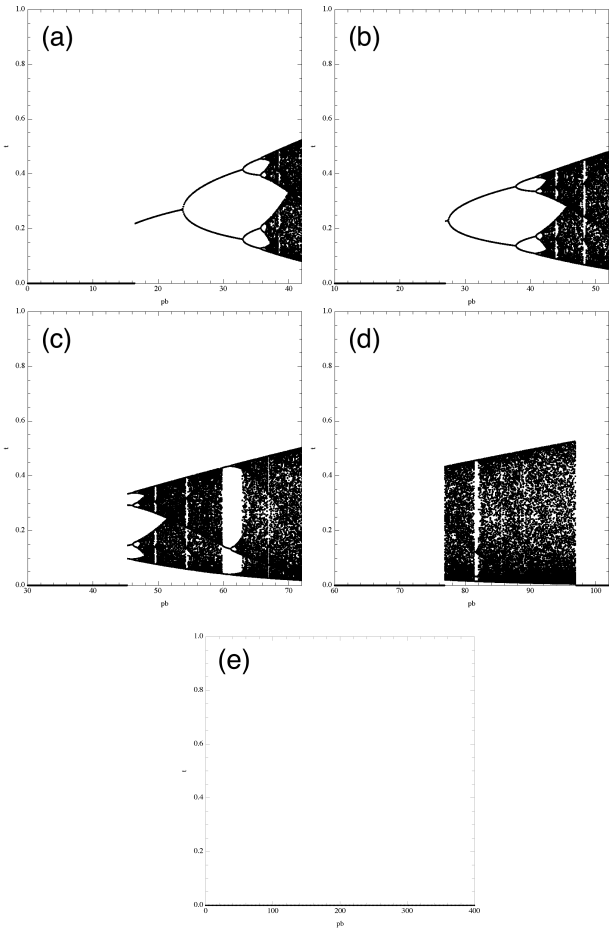

FIG. 8: Renormalization group topologies as p_b is scanned for $p_c = 0$ and (a) $p = 6$, (b) $p = 7$, (c) $p = 8$ (bifurcation truncation and direct transition into a 4-fold limit cycle), (d) $p = 9$ (absence of bifurcation and direct transition into the chaotic region) and (e) $p = 10$ (absence of bifurcations and chaos).

B. Alternating Reentrant Ferromagnetic and 'Pseudo' Spin-Glass Phases

Fig. 8(d) suggests that we should continue to probe even larger values of p_b. Let us now include both B- and C-terms and conduct a study within the restricted parameter space of $p_c = 1$, $p = 4$ and $dm = 1$, within which we will already see some interesting features. We do a p_b sweep for increasing values of m_1 beyond those originally considered and present the results in Figs. 9(a)-(c).

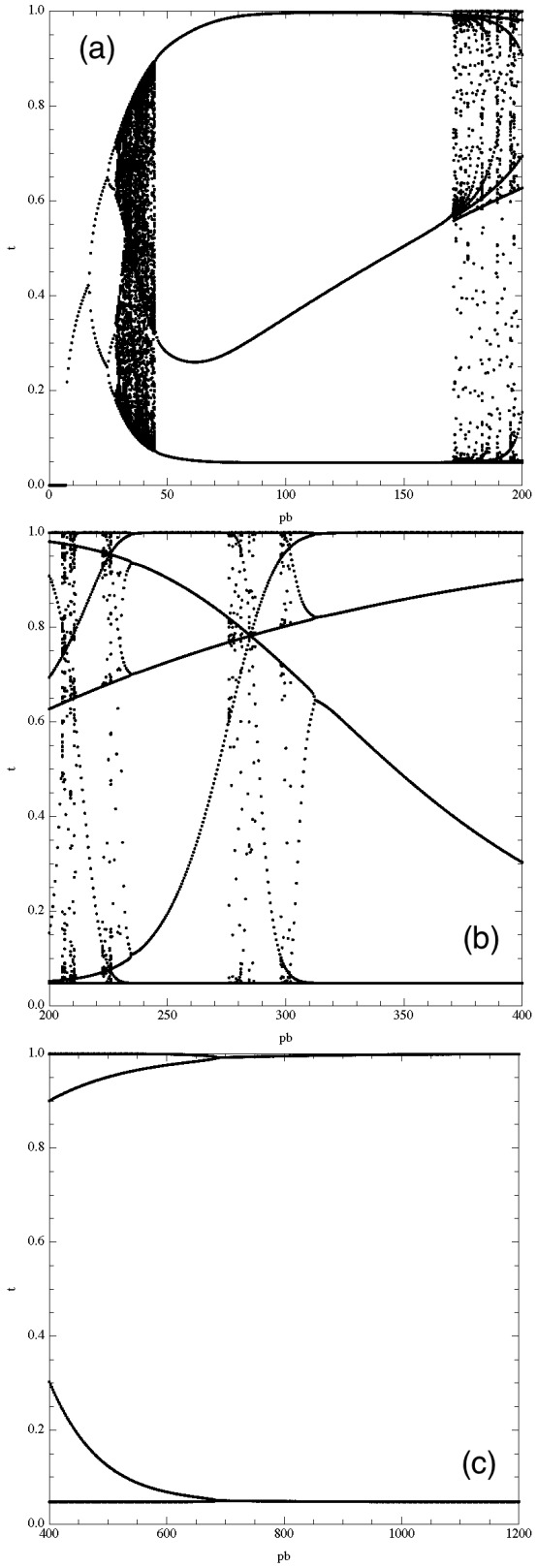

FIG. 9: Renormalization group topologies as p_b is scanned across different values for $p_c = 1$, $p = 4$, $dm = 1$, and $m_1 = 10$ with (a) $0 \leq p_b \leq 200$, (b)$200 \leq p_b \leq 400$, (c) $400 \leq p_b \leq 1200$. (a) and (b) shows alternating phase transitions between the FM and pseudo spin-glass phase beyond the initial spin-glass phase, and (c) shows the reverse bifurcation process and eventual settling into the FM phase.

For moderately small values of $m_1 = 10$, we see that at some sufficiently large value of p_b ($\simeq 45$), the spin-glass phase terminates and a 'reentrant' [1, 13] FM phase (period-3 limit cycle) takes over temporarily. Yet at higher p_b values ($\simeq 170$), a pseudo spin-glass phase takes over and by extending our p_b scan to even larger (potentially unrealistic) values, we see that there are a few alternating phase transitions between the reentrant FM and pseudo spin-glass phases [14], which eventually stabilizes into the FM phase via reverse bifurcation. Unlike the initial FM phase, the intriguing characteristic of these reentrant FM phases is that if we ignore effects of random noise from disorder, at different length scales, it alternates between infinitely strong coupling ($t \simeq 1$) and extremely weak coupling ($t \simeq 0.05$).Furthermore, the intermediate trajectories span almost the entire range of couplings through the various phase transitions. Without further detailed study, it is unclear which extreme the system will stabilize into with the inclusion of disorder sourced random noise, although intuitively, one would guess the answer to be the weak coupling FM phase, but that is assuming that the system will actually stabilize to either of them.

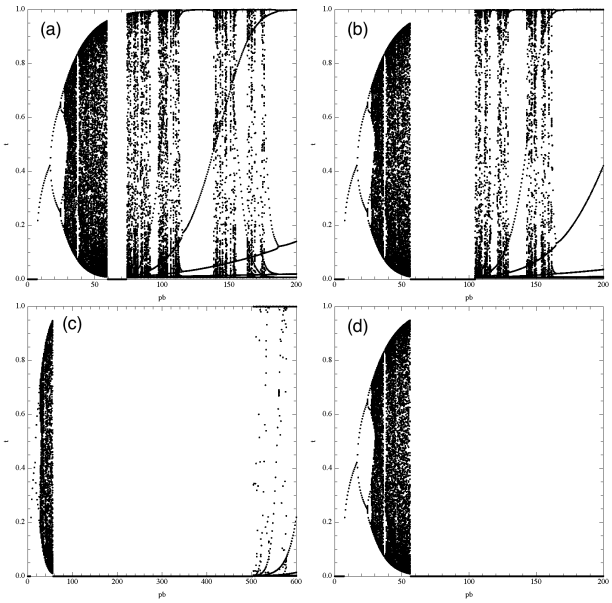

FIG. 10: Renormalization group topologies with $p_c = 1$ and $p = 4$ as p_b is scanned for increasing values of m_1 to show the growth in the intermediate reentrant paramagnetic phase. (a) $m_1 = 70$, (b) $m_1 = 100$, (c) $m_1 = 500$, (d) $m_1 \to \infty$ or equivalently, $p_c = 0$.

We mention in passing that for increasing values of m_1, the reverse bifurcation process finally stabilizes at increasing values of p_b. Such reverse bifurcation phenomena have been seen in other systems as well [15].

C. The Reentrant Paramagetic Phase and Its Stability

For yet larger values of m_1, a new interesting phenomenon emerges as we show in Figs. 10(a)-(d). An intermediate reentrant paramagnetic phase 'slips' into the spin-glass phase at moderately large m_1 ($\simeq 70$) and the range of p_b at which this reentrant paramagnetic phase is stable increases with increasing m_1 (i.e. for exponentially weaker contributions of the C-bonds). Only in the case where $m_1 \to 0$, or equivalently $p_c = 0$, do we see the reentrant paramagnetic phase being favored up to $p_b \to \infty$. This is consistent with the observation we showed in the first subsection, in particular, with Figs. 9(d) and 9(e), and supports the conclusion about the delicate nature of the spin-glass phase that we arrived at previously.
This was the subtlely that we hinted at the end of the previous section, where for non-zero p_c, even in some cases where $p_b \gg p_c$, the effects of the C-bonds, even when they are very weak, are still felt by the system. In fact, while in the absence of the C-bonds the high density of frustrated spin clusters p_b favors the disordered paramagnetic phase due to overfrustration, the C-bonds (even with miniscule influence) has a stabilizing effect that favours the spin-glass and FM ordering in the event of overfrustration.

V. CONCLUSION

We conclude that while many interesting features were stumbled upon in this study, the accuracy of the numerical results relies on how the limits of the various terms in the recursion relation were taken. We used Mathematica 8 for our study, during which underflow, overflow, and complex infinity errors have been common especially in the large m_1 and p_b limits, so that in order to overcome these issues, we had to manually enforce how some limits should be taken. Precision errors could also have an adverse effect on the chaotic regions but the regions with stable limit cycles and fixed points should be robust to these errors. It would be great to check these results on a different computational software or a more efficient and precise code. If truly the new results mentioned here hold up to other numerical checks, it would enrich the phase diagram originally proposed and the heighten the applicability of this class of models.

[1] S. R. McKay, A. N. Berker, and S. Kirkpatrick, "Spin-glass behavior in frustrated ising models with chaotic renormalization-group trajectories," *Phys. Rev. Lett.*, vol. 48, pp. 767–770, Mar 1982.

[2] R. B. Griffiths and M. Kaufman, "Spin systems on hierarchical lattices. introduction and thermodynamic limit," *Phys. Rev. B*, vol. 26, pp. 5022–5032, Nov 1982.

[3] See [4].

[4] We emphasise that for this scheme to be self-consistent, i.e. with $K \geq 0$ at every step of renormalization group transformation, we require $m_2 > m_1$. See discussion in Section III.

[5] There is a typographical error in the original paper, in which the authors stated that these plots were produced with $m_1 = m_2 + 1$ instead. We were not able to reproduce the plots with these parameters (as to be expected) as this violates the self consistency condition as per [4].

[6] R. Hilborn, *Chaos and Nonlinear Dynamics, 2nd Edition.* Oxford University Press, 2003.

[7] One could do the same with a reduced parameter space m_1 in the case of Fig. 2(c).

[8] N. m. c. Aral and A. N. Berker, "Chaotic spin correlations in frustrated ising hierarchical lattices," *Phys. Rev. B*, vol. 79, p. 014434, Jan 2009.

[9] J. Crutchfield and B. Huberman, "Fluctuations and the onset of chaos," *Physics Letters A*, vol. 77, no. 6, pp. 407 – 410, 1980.

[10] N. m. c. Aral and A. N. Berker, "Chaotic spin correlations in frustrated ising hierarchical lattices," *Phys. Rev. B*, vol. 79, p. 014434, Jan 2009.

[11] We have to be careful when taking this limit.

[12] H. C. Hsu, W.-L. Lee, J.-Y. Lin, B.-L. Young, H.-H. Kung, J. Huang, and F. C. Chou, "Spin-glass transition and giant paramagnetism in heavily hole-doped bi2sr2co2oy," *Journal of the Physical Society of Japan*, vol. 83, no. 2, p. 024709, 2014.

[13] A. N. Berker and J. S. Walker, "Frustrated spin-gas model for doubly reentrant liquid crystals," *Phys. Rev. Lett.*, vol. 47, pp. 1469–1472, Nov 1981.

[14] We denote this as a 'psuedo' spin glass phase because unlike the 'true' spin glass phase, the t points visited over repeated recursions are effectively limit cycles with large periods. They do not have the space filling property characteristic of chaotic trajectories. This is evident when we compare the density of points in this region to those of the 'true' spin-glass phase. A more detailed study can be done to determine the nature of this phase as well as its stability under random noise in real systems.

[15] J. Cascais, R. Dilo, and A. da Costa, "Chaos and reverse bifurcation in a {RCL} circuit," *Physics Letters A*, vol. 93, no. 5, pp. 213 – 216, 1983.